JOURNAL OF NATURAL PRODUCTS

pubs.acs.org/jnp

Article

Natural Isoflavones and Semisynthetic Derivatives as Pancreatic Lipase Inhibitors

Nunzio Cardullo,* Vera Muccilli, Luana Pulvirenti, and Corrado Tringali*

Cite This: *J. Nat. Prod.* 2021, 84, 654–665

Read Online

ACCESS | Metrics & More | Article Recommendations | Supporting Information

ABSTRACT: Obesity, now widespread all over the world, is frequently associated with some chronic diseases. Thus, there is a growing interest in the prevention and treatment of obesity. To date, the only antiobesity drug is orlistat, a natural product-derived pancreatic lipase (PL) inhibitor with some undesired side effects. In the last decades, many natural compounds or derivatives have been evaluated as potential PL inhibitors, and natural polyphenols are among the most promising for possible exploitation as antiobesity agents. However, few studies have been devoted to isoflavones. In this work, we report a study on the PL inhibitory properties of a small library of semisynthetic isoflavone derivatives together with the natural leads daidzein (**1**), genistein (**2**), and formononetin (**3**). In vitro lipase inhibition assay showed that **2** is the most promising PL inhibitor. Among synthetic isoflavones, the hydroxylated and brominated derivatives were more potent than their natural leads. Detailed studies through fluorescence measurements and kinetics of lipase inhibition showed that **2** and the bromoderivatives **10** and **11** have the greatest affinity for PL. Docking studies corroborated these findings highlighting the interactions between isoflavones and the enzyme, confirming that hydroxylation and bromination are useful modifications.

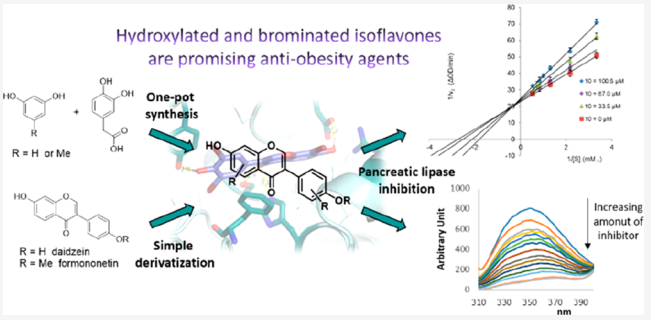

According to the World Health Organization (WHO) definition, overweight and obesity are defined as abnormal or excessive fat accumulation, and they present a risk to health. Although, in the past, obesity was frequently observed only in high income countries, now it is dramatically spreading also in low- and middle-income countries, particularly in urban settings. In 2016, 39% of both women and men aged 18 and over were overweight.[1] Leaving aside the aesthetic problems, which can cause psychological or social problems, obesity is a significant risk factor for a series of pathological conditions including cardiovascular diseases, hypertension, hyperlipidemia, diabetes, mental disorders, and some forms of cancer.[2,3] Thus, prevention and treatment of obesity have attracted the attention of many individual researchers and health organizations. Of course, physical exercise and a carefully balanced diet are the first prerequisites for fighting obesity. However, they often do not solve the problem, and therefore, it is necessary to employ specific therapies. Because liposuction is a surgical treatment (not without risk) giving satisfactory results only in some cases,[2] the main recently adopted therapies have been based essentially on three drugs, namely, orlistat (Xenical), a natural product-derived inhibitor of pancreatic lipase (PL, triacylglycerol acyl hydrolase), sibutramine (Reductil), and rimonabant (Acomplia), the latter two are both appetite suppressants, acting with different mechanisms.[4] Nevertheless, sibutramine and rimonabant have been withdrawn from the market due to major adverse cardiovascular events and significant psychiatric undesired effects, respectively.[5,6] Thus, orlistat remains the only drug on the market to treat obesity, although it shows unpleasant gastrointestinal side effects.[6,7] This situation prompted many research groups to search for new, effective, and safe drugs to treat obesity, and several potential antiobesity drugs are currently in clinical trials. In this scenario, PL inhibitors play a major role: PL normally hydrolyzes 50−70% of total dietary fats;[4] the interaction of inhibitors with the enzyme causes the blocking of its catalytic activity, which is the hydrolysis of triglycerides, thus reducing the intestinal fat absorption, and the consequent accumulation of adipose tissue. PL inhibitors are normally excreted with the enzyme, causing no long-term effects, and are generally regarded as relatively safe.[2]

In the search for new PL inhibitors, a special focus has been devoted to natural compounds or derivatives, in consideration of the number and the variety of plants and microorganisms producing metabolites with potential antiobesity activity.[4,5,8]

Special Issue: Special Issue in Honor of A. Douglas Kinghorn

Received: December 28, 2020
Published: March 1, 2021

Moreover, many natural products show low absorption rates, and this generally reduces systemic adverse effects.[9] These natural inhibitors may also be considered as lead compounds to obtain, through chemical modification, optimized products with enhanced properties, but they maintain low or absent toxicity. Orlistat itself is a semisynthetic compound derived from the natural product lipstatin, an unusual β-lactone originally isolated from the actinomycete *Streptomyces toxytricini*.[10−12]

Previously reported natural inhibitors belong to various chemical classes, including carbohydrates, saponins, terpenes, and polyphenols; also, polyphenol-rich extracts are reported for PL inhibition,[4] and some phenolics have showed multifunctional antiobesity properties.[8] Thus, polyphenols are among the most promising natural products for possible exploitation as antiobesity agents. A significant number of polyphenolic compounds with PL inhibitory activity have been reported, including flavonoids, phenolic acids, lignans, the stilbenoid resveratrol, and proanthocianydins.[3,7,13] Nevertheless, less attention has been devoted to some polyphenol subfamilies, such as isoflavones. These natural products are well-known for other beneficial properties, mainly as phytoestrogenic,[14] anti-inflammatory,[15] cancer chemopreventive,[16] antioxidative, antidiabetic,[17] and neuroprotective agents.[18] The PL inhibitory activity of the isoflavones daidzein (**1**) and genistein (**2**) has been reported,[19] but no data are available for their mechanism of action nor for isoflavone derivatives.

Furthermore, it is noteworthy here that, in recent years, the beneficial effect of soy products in preventing metabolic disorders, including hyperlipidemia, have been reported. These properties have been attributed to the high levels of isoflavones in soy (as well as of proteins, fibers, and unsaturated fats).[20] In some clinical trials, the effect of soy or soy isoflavones consumption on weight and other obesity-related pathologies has been examined, concluding that soy is a suitable food for antiobesity effects.[21] More in detail, the antiobesity action of isoflavones is imputable, on one hand, to inhibition of lipogenesis and to the increase of fatty acid β-oxidation[22] and, on the other hand, to regulation of food intake and energy expenditure, as well as in prevention of fat accumulation in adipose tissue.[21]

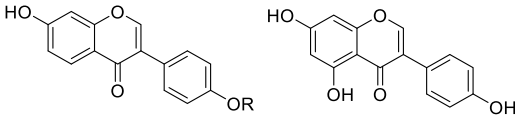

On this basis, as a continuation of our study on the search of bioinspired polyphenols capable of inhibiting enzymes involved in metabolic diseases,[23−25] we report herein the PL inhibitory properties of a small library of natural isoflavones and semisynthetic derivatives.

RESULTS AND DISCUSSION

As the first step of this study, we planned to obtain a small library of natural and semisynthetic isoflavones from daidzein (**1**), genistein (**2**), and formononetin (**3**) and to evaluate these compounds as PL inhibitors. Unfortunately, attempts to obtain genistein derivatives were unsuccessful (experimental details are listed in the Supporting Information). Further steps were devoted to in vitro lipase inhibition assays, fluorescence spectra measurements, kinetics of lipase inhibition, and docking studies, as detailed in the following.

Synthesis. In the present work, a metal-free synthetic methodology has been adopted to afford isoflavone analogues with an *ortho*-dihydroxylated aromatic ring (catechol group). This approach consists of the preparation of deoxybenzoin from respective substituted phenol and phenyl acetic acid precursors by Friedel−Crafts acylation and the use of Vilsmeier reagent [*N*,*N*′-dimethyl(chloromethylene)-ammonium chloride] formed from methyl sulfonyl chloride and DMF. This route is very effective for converting deoxybenzoins into corresponding isoflavones with mild reaction conditions, short reaction times, and excellent yields.[26,27] More specifically, in a two-step procedure, a deoxybenzoin intermediate was obtained by reaction of resorcinol (**4**) or orcinol (**5**) with 3,4-dihydroxyphenylacetic acid (**6**), in the presence of $BF_3{\cdot}Et_2O$. The intermediates were subsequently treated with the Vilsmeier reagent in the presence of $BF_3{\cdot}Et_2O$ (Scheme 1a), thus affording, respectively, **7** and **8**. In other experiments, we also carried out a one-pot synthesis, directly treating the intermediates with Vilsmeier reagent to afford **7** and **8** (Scheme 1b).

Scheme 1. (a) Two-Step and (b) One-Pot Synthesis of Isoflavones 7 and 8

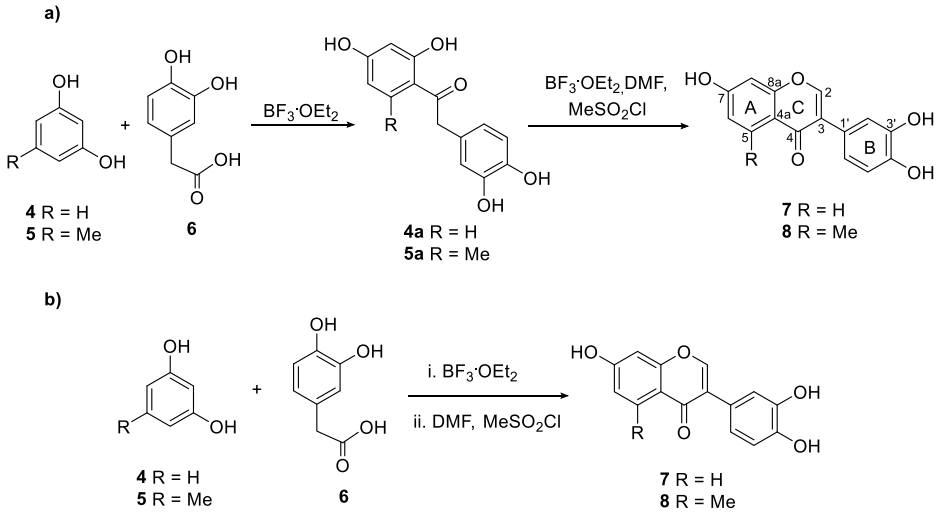

https://dx.doi.org/10.1021/acs.jnatprod.0c01387
J. Nat. Prod. 2021, 84, 654−665

Table 1 reports the reaction conditions for both two-step (entries 1−3) and one-pot (entries 4 and 5) syntheses with the respective reaction yields.

Table 1. Reaction Conditions for the Synthesis of 7 and 8

entry	R	$BF_3{\cdot}OEt_2$	T (°C)	overall yield (%)[a]
		Two-Step		
1	H	12 equiv	110[b]	42
			80[c]	
2	H	8 equiv	110[b]	57
			80[c]	
3	Me	8 equiv	110[b]	16
			80[c]	
		One-Pot[d]		
4	H	7.5 equiv	i. 110	94
			ii. 80	
5	Me	7.5 equiv	i. 110	37
			ii. 80	

[a]The yield was determined after precipitation or liquid chromatography purification. [b]Temperature of the first step of the reaction. [c]Temperature of the second step of the reaction. [d]See Scheme 1b for details.

The one-pot method allows obtaining higher yields and requires lower equivalents of $BF_3{\cdot}Et_2O$; thus, the one-pot method was preferred for preparative syntheses. Of note, this method afforded the natural isoflavone **7** with 94% yield, far higher than previously reported in the literature.[28]

The previously unreported isoflavone **8** was subjected to spectroscopic characterization by HRMS and 1D and 2D NMR spectroscopy. The assignments of ^1H and ^{13}C NMR signals are listed in Table 2, and HRMS data are reported in the Experimental Section. The presence in the ^1H NMR spectrum of the distinctive singlet at δ 8.19 (H-2) is indicative of the formation of ring C and therefore of an isoflavone. The key HMBC correlation of H-2 with the signals at δ 176.5 (C-4), 158.8 (C-8a), and 124.4 (C-1′) confirmed the isoflavone skeleton and allowed the reported assignments. The signals at δ 7.13 (bs), 7.02 (d, J = 8.5 Hz), and 6.97 (d, J = 8.5 Hz) have been assigned respectively to H-2′, H-6′, and H-5′ of ring B. The broad singlets at δ 6.67 and 6.70 are attributable to the protons of ring A. HSQC correlations allowed the assignments of CH sp^2 carbons, as reported in Table 2. The carbon signals at δ 116.9 and 100.0 couple with the proton signals at δ 6.67 and 6.70, respectively; however, their unambiguous assignment as CH-6 and CH-8 was only possible after the analysis of the HMBC correlations. Namely, the signal at δ 6.70 (H-8) showed key correlations with the carbons at δ 161.0 (C-7) and 158.8 (C-8a). Analogously, the signal at δ 6.67 (H-6) was long-range correlated with the bridged carbon at δ 114.7 (C-4a) and the methyl carbon a δ 22.9. This latter correlation was pivotal to establish the C-5 position for the methyl group in isoflavone **8**. The phenolic OH signal at δ 10.62 was positioned at C-7 on the basis of key correlations with the deshielded nonprotonated carbon at δ 161.0 (C-7) as well as with the carbon signals of C-8 and C-6.

Table 2. ^1H (500 MHz) ^{13}C (125 MHz) and HMBC NMR Data of 8 in DMSO-d_6

position	δ_C, type	δ_H, multiplet (mult.) (J in Hz)	HMBC[a]
2	151.9, CH	8.19, s	4, 8a, 1′
3	124.8, C		
4	176.4, C		
4a	114.7, C		
5	142.2, C		
6	116.9, CH	6.67, bs	4a, 5-Me
7	161.0, C	10.62, s (OH)	6, 7, 8
8	100.0, CH	6.70, bs	7, 8a
8a	158.8, C		
1′	124.4, C		
2′	115.4, CH	7.13, bs	3, 4′, 6′
3′	147.6, C		
4′	147.9, C	8.31, s (OH)	
5′	112.7, CH	6.97, d (8.5)	1′, 3′
6′	121.0, CH	7.02, d (8.5)	3, 2′, 4′
5-Me	22.9, CH_3	2.70, s	4a, 5, 6

[a]HMBC correlations are from proton(s) stated to the indicated carbon.

To obtain further isoflavone analogues, we resorted to simple reactions, namely, *ortho*-hydroxylation and bromination of the natural isoflavones daidzein (**1**) and formononetin (**3**). The corresponding catechol derivatives were prepared employing the hypervalent iodine reagent 2-iodoxybenzoic acid (IBX). The optimization of this reaction (Table S1, Supporting Information) suggested the use of different conditions for each substrate. According to literature findings on similar compounds,[29] the *ortho*-hydroxylation of daidzein should have afforded products with a catechol group on ring A, ring B, or both. Nevertheless, in the reported conditions (Scheme 2a), only one major compound was obtained, subsequently identified as the isoflavone **7**. The *ortho*-hydroxylation of formononetin afforded the natural isoflavone retusin (**9**)[26] with 43% yield (Scheme 2b).

Scheme 2. Selective Hydroxylation of (a) 1 and (b) 3

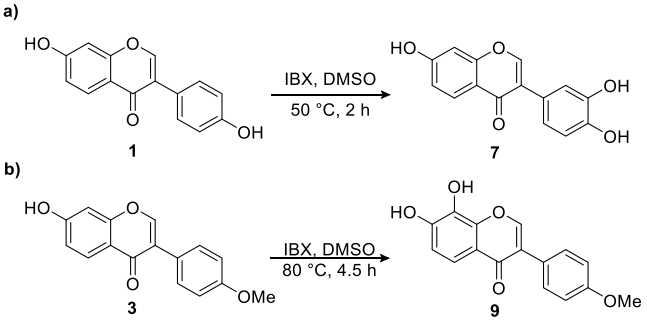

Also the preparation of the brominated analogues required an optimization step, as summarized in Table 3. The experiments were performed mainly on formononetin (**3**), and the results suggested the conditions to be employed for daidzein (**1**). Two brominating reagents, namely, NaBr in the presence of oxone or H_2O_2 and Br_2, were employed in different solvents and at various temperatures.

The isoflavones **1** and **3** reacted appreciably only with bromine (entries 3−5). The syntheses were scaled-up according to the best reaction conditions, as reported in Scheme 3. Although a diluted Br_2 solution was gradually added to daidzein and the reaction was maintained at 0 °C (Scheme 3a), **1** gave exclusively 8,3′,5′-tribromodaidzein (**10**) with 70% yield. By treating **3** under the same conditions, only 8-bromoformononetin (**11**) was recovered with 80% yield

https://dx.doi.org/10.1021/acs.jnatprod.0c01387
J. Nat. Prod. 2021, 84, 654−665

Table 3. Reaction Conditions for the Synthesis of 10−12

entry	isoflavone	solvent	brominating agent (1.2 equiv)	T (°C)	time	yield (%)[a]
1	**3**	CH_3COOH	NaBr, H_2O_2	rt	6 h	3
2	**3**	CH_3COOH	NaBr, oxone	rt	6 h	8
3	**3**	CH_3COOH	Br_2 in CH_3CN	rt	40 min	92
4	**3**	$CHCl_3$, MeOH[b]	Br_2 in $CHCl_3$	0	1 h	80
5	**1**	$CHCl_3$, MeOH[b]	Br_2 in $CHCl_3$	0	3 h	67

[a]After the completion of reaction, a saturated solution of $Na_2S_2O_3$ was added to reduce the excess of halogenating agent. The yield of the product was determined after isolation by liquid−liquid partition, or when necessary, after purification by liquid chromatography. [b]Employed in a small amount to solubilize the isoflavone, see Experimental Section.

Scheme 3. Synthesis of Brominated Isoflavones 10−12

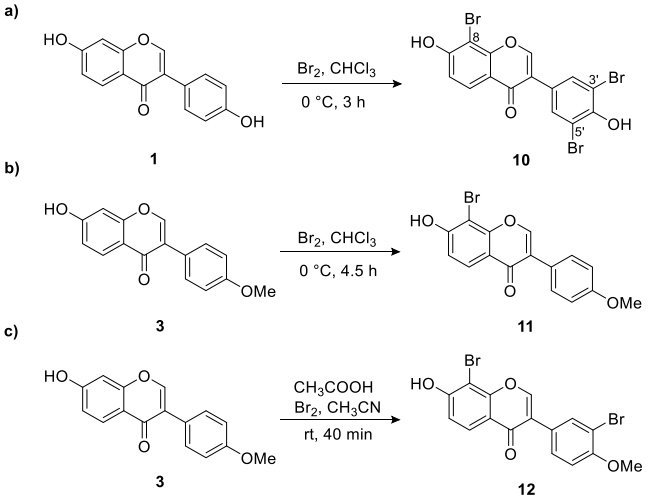

(Scheme 3b). When **3** was dissolved in acetic acid and a bromine solution was slowly added at room temperature, 8,3′-dibromoformononetin (**12**) was obtained with 92% yield (Scheme 3c).

The new brominated isoflavones **11** and **12** were subjected to spectroscopic characterization by HRMS spectrometry and 1D and 2D NMR spectroscopy. The assignments of ^1H and ^{13}C NMR signals are listed in Table 4, and HRMS data are reported in the Experimental Section. The brominated isoflavone **10** has been obtained very recently from daidzein as a biotransformation product by *Actinomadura* sp. RB99; it has been named maduraktermol H.[30]

To establish if isoflavones without free phenolic groups could inhibit PL, the isoflavone **7** was subjected to methylation and acetylation to obtain, respectively, its permethylated derivative, the natural product cabreuvine (**13**),[31] and its peracetylated derivative **14** (Scheme 4). Although **14** has been previously reported,[32] its NMR data have not been tabulated; therefore, they are listed in Table 4.

In Vitro Lipase Inhibitory Activity. The natural isoflavones **1**−**3**, together with the synthesized products **7**−**14**, were studied as potential pancreatic lipase (PL) inhibitors. A spectrophotometric methodology employing 4-nitrophenyl butyrate as a substrate for the PL was applied.[33] The results of the in vitro assay are reported in Table 5 as IC_{50} values; the commercial antiobesity drug, orlistat, was employed as a positive control.

Table 4. ^1H (500 MHz) and ^{13}C (125 MHz) NMR Data of 11, 12, and 14

	11[a]		**12**[b]		**14**[b]	
position	δ_C, type	δ_H, mult. (J in Hz)	δ_C, type	δ_H, mult. (J in Hz)	δ_C, type	δ_H, mult. (J in Hz)
2	153.9, CH	8.50, s	152.8, CH	7.98, s	153.4, CH	7.98, s
3	123.7, C		123.6, C		123.9, C	
4	174.8, C		175.9, C		175.2, C	
4a	117.9, C		118.0, C		122.2, C	
5	126.3, CH	7.97, d (8.8)	126.2, CH	8.01, d (8.8)	127.8, CH	8.26, d (8.8)
6	115.0, CH	7.12, d (8.8)	114.3, CH	6.96, d (8,8)	119.6, CH	7.13, d (8.8)
7	160.2, C		159.7, C	8.30, bs (OH)	154.0, C	
8	97.1, C		97.0, C		110.9 CH	7.26, bs
8a	154.5, C		155.3, C		156.5, C	
1′	124.2, C		125.1, C		130.3, C	
2′	130.6, CH	7.52, d (8.6)	133.6, CH	7.68, d (2.2)	124.0, CH	7.41, bs
3′	114.1, CH	6.99, d (8.6)	111.6, C		141.0, C	
4′	159.5, C		156.0, C		142.0, C	
5′	114.1, CH	7.52, d (8.6)	111.9, CH	6.92, d (8.5)	123.4, CH	7.21, d (8.5)
6′	130.6, CH	6.99, d (8.6)	129.6, CH	7.42, dd (2.2, 8.5)	126.8, CH	7.39, d (8.5)
4′-OMe	55.6, CH_3	3.78, s	56.2, CH_3	3.86, s		
3′/4′−OCO					168.1, C	
7−OCO					168.4, C	
3′/4′−OCOMe					20.6, CH_3	2.25, s
7−OCOMe					21.1, CH_3	2.30, s

[a]NMR spectra were run in DMSO-d_6. [b]NMR spectra were run in chloroform-*d*.

https://dx.doi.org/10.1021/acs.jnatprod.0c01387
J. Nat. Prod. 2021, 84, 654−665

Scheme 4. Synthesis of Cabreuvine (13) and of Isoflavone 14

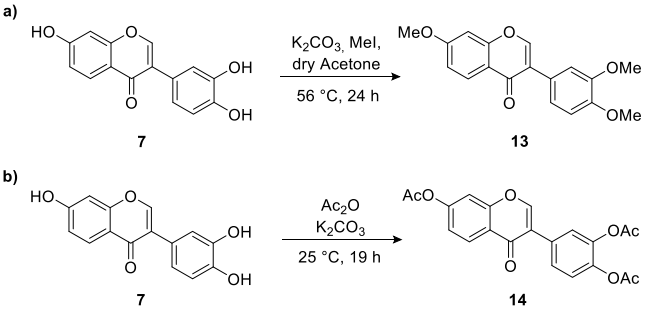

Table 5. PL Inhibitory Activity (IC_{50}) of Isoflavones 1−3 and 7−14

compound	IC_{50} ± SD (μM)[a]
1	83 ± 1
2	60 ± 5
3	120 ± 6
7	70 ± 3
8	92 ± 2
9	93 ± 14
10	63 ± 4
11	87 ± 8
12	100 ± 10
13	360 ± 10
14	122 ± 10
orlistat	0.6 ± 0.1

[a]Results are reported as mean ± SD (n = 3).

Daidzein (**1**) and genistein (**2**) showed promising PL inhibitory activity when compared with the natural formononetin (**3**); of note, compounds **7** and **9**, corresponding to the hydroxylated derivatives of daidzein and formononetin, respectively, proved to be more active inhibitors than the natural leads. More in detail, the position and the number of hydroxy groups is determinant for the PL inhibitory activity. Namely, the insertion of an OH either into ring A (as in **9**) or into ring B (as in **7**), in *ortho* position to phenolic moiety, increases the activity, and the loss of the OH at C-5 (as in **2** with respect to **1**) diminishes the efficacy. In compound **8** the insertion of a methyl group at C-5 was detrimental for the activity, as highlighted by comparison with **7**. The OH at C-4′ seems to be important for PL inhibition, as can be observed comparing **3** with **1**, and more generally, the lack of free OH groups is highly detrimental for the activity, as shown by the data on the permethylated **13** and peracetylated **14**, with respect to the parent compound **7**. Also bromination proved to be an effective modification for improving the PL inhibitory activity. In particular, the most potent synthetic compound obtained in this study was 8,3′,5′-tribromodaidzein (**10**), significantly more active than its natural lead **1**. Similarly, 8-bromoformonetin (**11**) and 8,3′-dibromoformonetin (**12**) were more active than **3**. Within brominated isoflavones, we could not find a clear structure−activity relationship between number and position of the bromine atoms and their inhibitory capacity. The structure−activity relationships described above are graphically summarized in Figure 1. These encouraging results prompted us to carry out further experiments on selected isoflavones, as detailed in the following sections.

Fluorescence Spectra Measurements. According to literature data, there are 7 Trp, 25 Phe, and 16 Tyr residues in pancreatic lipase that may be responsible for the fluorescence emission of this protein.[9] Changes in the fluorescence intensity of PL are attributed to the interaction with ligands which can modify the polarity of the environment surrounding the Trp residues, although changes in the environment of Phe and Tyr residues also give a minor contribution to fluorescence quenching. Intrinsic fluorescence experiments were performed to evaluate possible PL−isoflavone interactions. Thus, fluorescence spectra of PL were recorded upon the addition of different aliquots of the natural isoflavones **1**−**3**, as well as of the synthetic products **10** and **11**, showing promising inhibitory activity. The measurements were carried out at three different temperatures, namely, 27, 32, and 37 °C, and showed that the PL fluorescence intensity decreases with increasing concentrations of all compounds under study (Figures S31−S35). A slight bathochromic shift of the maximum fluorescence intensity (from 350 to 362 nm) was observed in all the titrations. The decrease in fluorescence intensity accompanied by a bathochromic shift has been reported to be related with an increase in the polarity environment surrounding the Trp residues, probably due to a conformational transition of the protein caused by the interaction between these isoflavones and PL.[9,34]

The data obtained from fluorescence titrations were analyzed according to the Stern−Volmer equation (eq 2), and the results were plotted as depicted in Figures 2 and 3 to gain some information on the mechanism of quenching. The

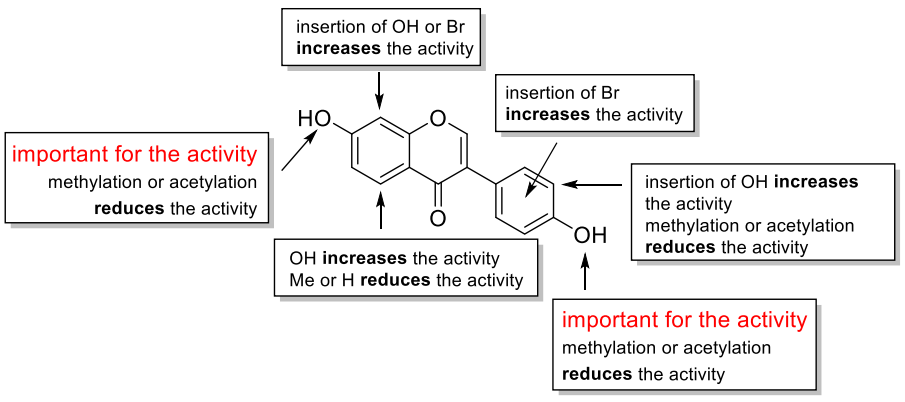

Figure 1. Structural features affecting the PL inhibitory activity of isoflavones.

https://dx.doi.org/10.1021/acs.jnatprod.0c01387
J. Nat. Prod. 2021, 84, 654−665

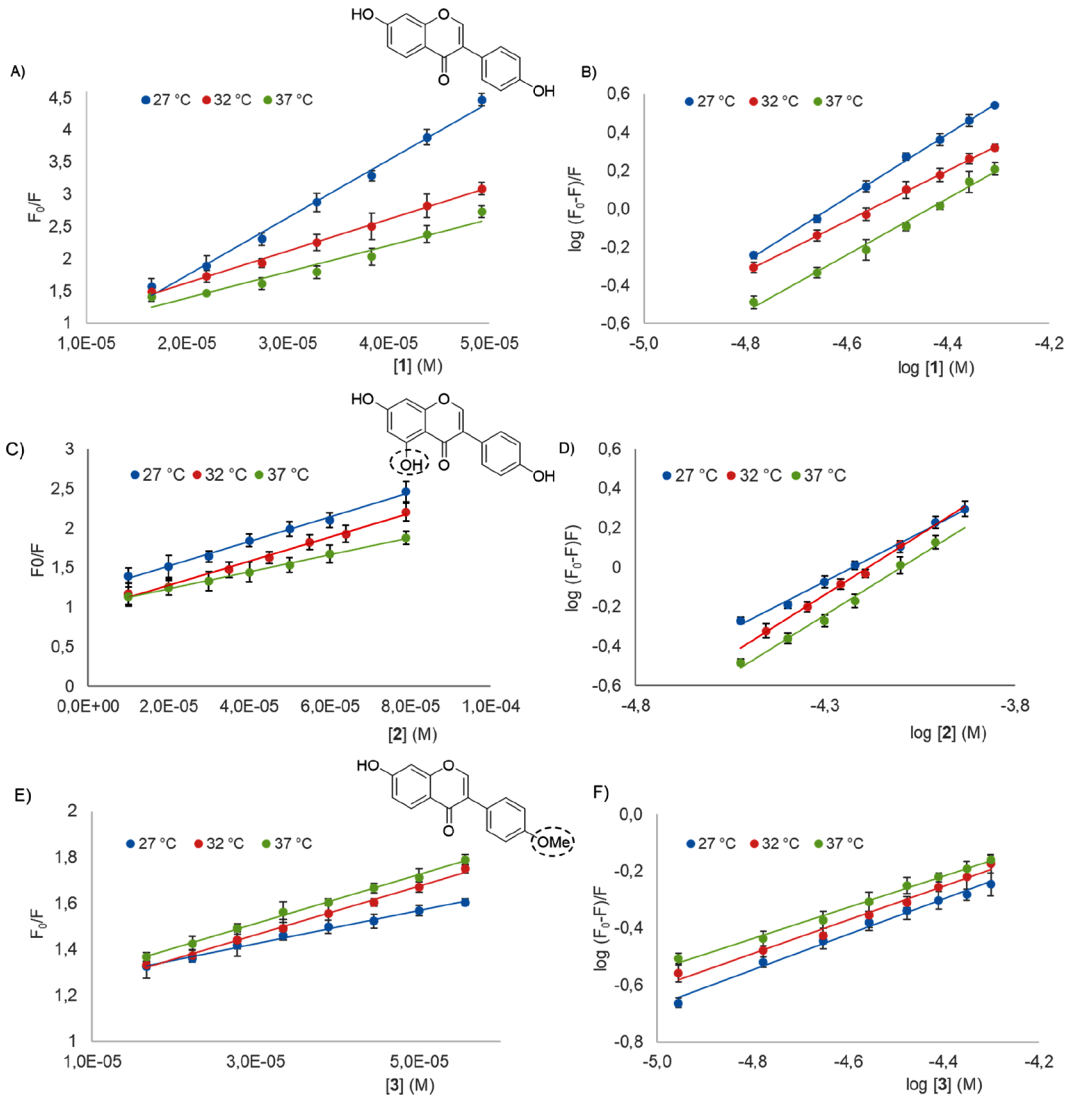

Figure 2. Stern–Volmer plots for the interaction of PL with (A) daidzein (**1**), (C) genistein (**2**), and (E) formononetin (**3**). Double log Stern–Volmer plots of PL with (B) **1**, (D) **2**, and (F) **3**. Each line was obtained with data of three independent experiments.

linearity observed by plotting F_0/F and [Q] (Figures 2 and 3) allowed determination of the existence of a single quenching process, static or dynamic. Table 6 summarizes the K_{sv} and K_q values for the PL–isoflavone interactions. As shown in Table 6, K_{sv} values decrease as the temperature increases for daidzein (**1**), genistein (**2**), and the bromoderivative **11** suggesting that fluorescence quenching occurs with a static mechanism.[35] Indeed, the rate constant values (K_q) obtained are greater than the typical values reported for collisional diffusion processes (2.0×10^{10}), confirming the occurrence of static quenching.[36] The data obtained for formononetin (**3**) and tribromodaidzein (**10**) suggest a different behavior, and in particular, the increase of K_{SV} and rate constant values with increasing temperature is indicative of a dynamic quenching process.

Further parameters useful to study the interactions of isoflavones with PL, namely the binding constant (K_a) and the number of binding sites per enzyme molecule (n) were obtained plotting eq 3 (Figures 2 and 3). These values are reported in Table 6. The K_a value is inversely correlated with the temperature for isoflavones **1**, **2**, and **11**, corroborating the assumption of a static quenching based on K_{SV} variation, whereas the K_a value of **3** and **10** increases with temperature, as expected for a dynamic quenching. The highest K_a values at 37 °C were obtained for the bromoderivatives **10** and **11**, suggesting a greater affinity for PL for these isoflavones.

Kinetics of Lipase Inhibition. The inhibition of pancreatic lipase by selected isoflavones was also evaluated through an enzyme kinetics study. As detailed in the Experimental Section, the mode of inhibition by compounds **1–3**, **10**, and **11** on PL was determined through the Lineweaver–Burk graphs, by plotting the reciprocal of initial velocity (v_0) versus the reciprocal of substrate concentration (Figure 4).

These plots showed that all of the tested isoflavones, except genistein (**2**), act as mixed-type inhibitors of PL, exhibiting both competitive and noncompetitive mechanisms. Namely, **1**, **3**, **10**, and **11** compete with the employed substrate for binding to PL, but they could also bind to the PL–substrate complex. Differently, **2** inhibits the PL activity in a competitive manner. The secondary plots of the y-intercept and slope, against the isoflavones concentration, were linearly fitted, indicating a single class of inhibition sites or a single inhibition site between PL and the tested isoflavones. The K_i

https://dx.doi.org/10.1021/acs.jnatprod.0c01387
J. Nat. Prod. 2021, 84, 654–665

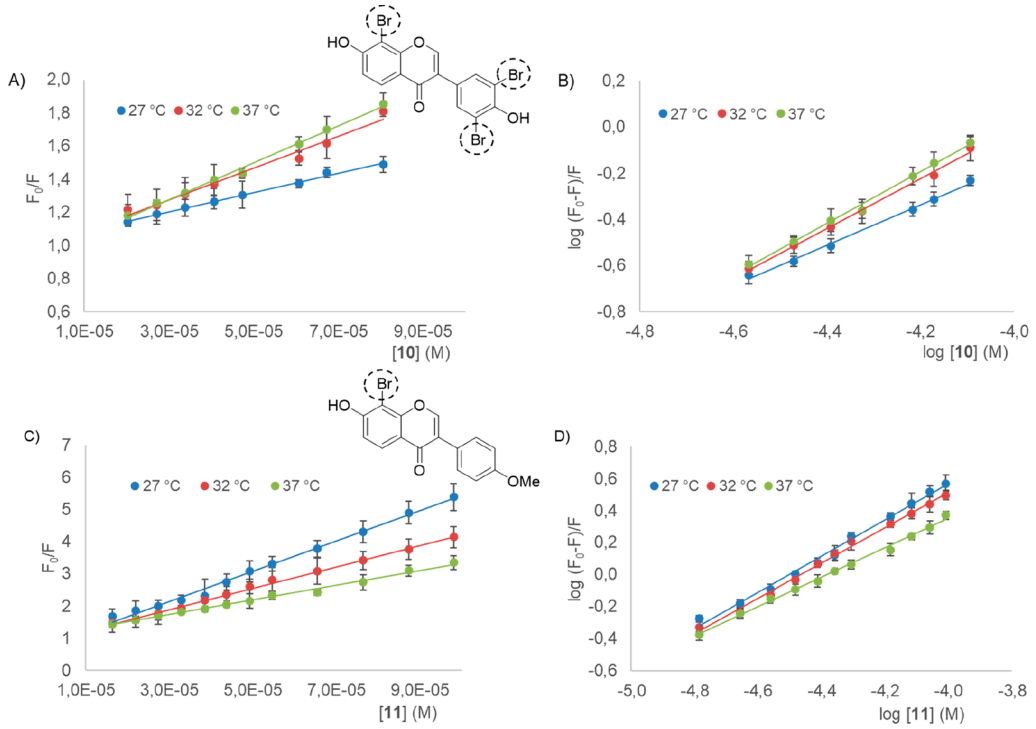

Figure 3. Stern−Volmer plots for the interaction of PL with (A) **10** and (C) **11**. Double log Stern−Volmer plots of PL with (B) **10** and (D) **11**. Each line was obtained with data of three independent experiments.

Table 6. K_{SV}, K_q, K_a, and n Values of the Interaction Between PL and Selected Isoflavones

	T (°C)	K_{SV} (×10^4 L/mol)	K_q (×10^{13} L/mol s)	R^2	K_a (×10^4 L/mol)	n	R^2
1	27	8.95 ± 0.32	5.62 ± 0.32	0.9921	5.30 ± 0.67	1.66	0.9986
	32	4.94 ± 0.41	3.11 ± 0.41	0.9968	1.20 ± 0.12	1.36	0.9981
	37	4.08 ± 0.62	2.57 ± 0.62	0.9992	1.02 ± 0.17	1.43	0.9914
2	27	1.88 ± 0.05	1.18 ± 0.05	0.9938	1.24 ± 0.52	1.20	0.9971
	32	1.50 ± 0.11	0.94 ± 0.11	0.9907	0.87 ± 0.21	1.16	0.9977
	37	1.07 ± 0.07	0.67 ± 0.07	0.9971	0.44 ± 0.07	1.03	0.9922
3	27	0.72 ± 0.02	0.45 ± 0.02	0.9935	0.16 ± 0.04	0.62	0.9908
	32	1.02 ± 0.03	0.64 ± 0.03	0.9976	0.22 ± 0.04	0.59	0.9913
	37	1.06 ± 0.08	0.66 ± 0.08	0.9937	0.27 ± 0.01	0.55	0.9929
10	27	0.58 ± 0.02	0.36 ± 0.02	0.9937	0.32 ± 0.08	0.87	0.9945
	32	0.96 ± 0.04	0.60 ± 0.04	0.9903	1.99 ± 0.14	1.05	0.9900
	37	1.11 ± 0.06	0.70 ± 0.06	0.9955	3.21 ± 0.72	1.12	0.9968
11	27	4.69 ± 0.17	2.95 ± 0.17	0.9931	12.4 ± 0.71	1.14	0.9920
	32	3.34 ± 0.08	2.10 ± 0.08	0.9967	8.47 ± 0.56	1.09	0.9957
	37	2.29 ± 0.11	1.43 ± 0.11	0.9924	1.47 ± 0.26	0.91	0.9962

values (related with the competitive mechanism) determined for **1**, **3**, **10**, and **11**, were lower than K'_i values (related with the noncompetitive mechanism), thus implying that these isoflavones could bind much tighter to the PL catalytic site than to the PL−substrate complex. Moreover, a very good correlation between K_i and IC_{50} values was observed (R^2 = 0.9963), corroborating the results about a promising PL inhibitory activity of isoflavones and, particularly, of genistein (**2**) and tribromodaidzein **10**.

Molecular Docking Study. A molecular docking study was carried out to determine the affinity of the isoflavones **1**−**3** and **7**−**14** for the pancreatic lipase catalytic site and their preferred orientation. This could also allow a better understanding of the inhibition mechanism. The binding site of PL includes the following residues: Ser152, Phe215, Arg256, His263, Leu264, Asp176, and Tyr114. The computational experiments were acquired employing Autodock4 and Autodock Vina (see the Experimental Section for more details).[37−39]

The docking outcomes showed that all of the ligands are well accommodated into the binding pocket, occupying almost an equivalent spatial portion of the cavity. The calculated binding energy (kcal/mol), listed in Table S2, suggests a promising affinity of this class of inhibitors, also confirmed by visual inspection of docked conformations; a list of molecular interactions for each analyzed compound is reported in the Supporting Information (Table S3).

The observation of docking poses showed that the isoflavone skeleton accommodates into the binding site and also highlighted that the compounds under study are able to establish noncovalent interactions with His263, His151, Ser152, Asp79, Pro180, Gly76, and Tyr114 of catalytic

https://dx.doi.org/10.1021/acs.jnatprod.0c01387
J. Nat. Prod. 2021, 84, 654−665

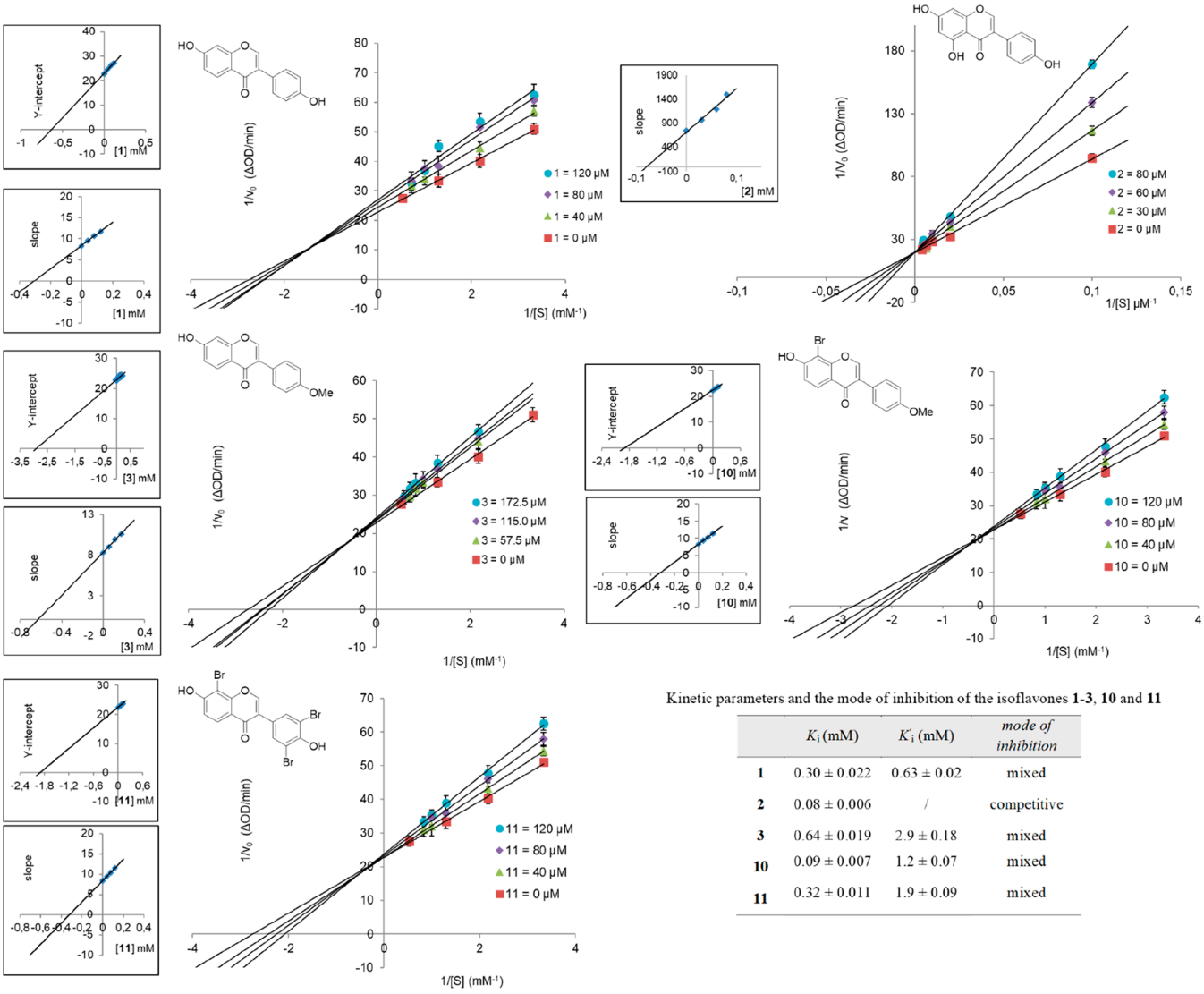

Kinetic parameters and the mode of inhibition of the isoflavones **1**-**3**, **10** and **11**

	K_i (mM)	K'_i (mM)	*mode of inhibition*
1	0.30 ± 0.022	0.63 ± 0.02	mixed
2	0.08 ± 0.006	/	competitive
3	0.64 ± 0.019	2.9 ± 0.18	mixed
10	0.09 ± 0.007	1.2 ± 0.07	mixed
11	0.32 ± 0.011	1.9 ± 0.09	mixed

Figure 4. Lineweaver−Burk plots of isoflavones **1**−**3**, **10**, and **11** with PL. The secondary inset plots represent slope versus [I] and *y*-intercept versus [I].

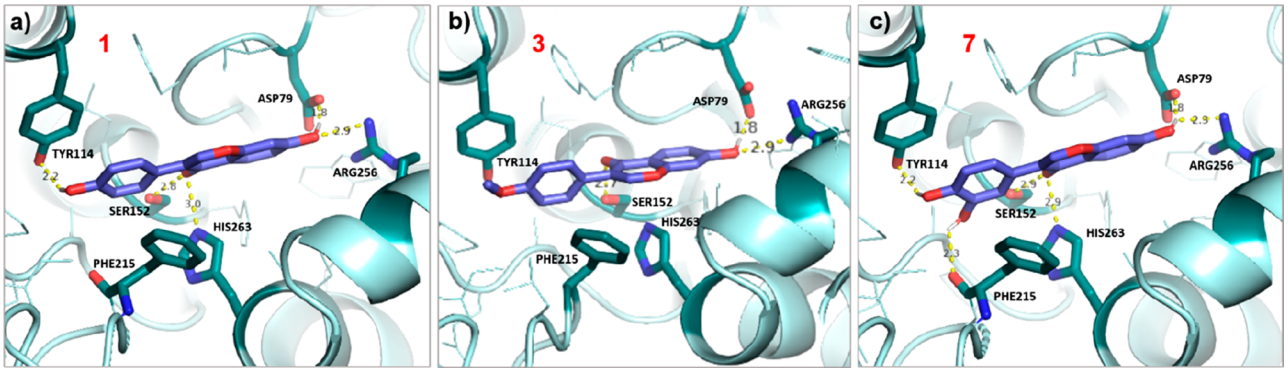

Figure 5. (a) Daidzein (**1**), (b) formononetin (**3**), and (c) isoflavone 7 into the binding site of PL; the residues of PL structure were represented using stick structures. The labeled dashes lines (yellow) represent hydrogen-bonding interactions.

pocket. Among the natural isoflavones, daidzein (**1**) and genistein (**2**) showed the best fitting in terms of intermolecular interactions with PL, if compared with formononetin (**3**). In particular, the pose of **1** (Figure 5a) into the cavity shows that the OH at C-7 interacts with both Arg256 and Asp79; the oxygen of the ketone function is involved in two hydrogen bonds with His263 and Phe215, and the OH at C-4′ establishes a hydrogen bond with Tyr114. In genistein (**2**), the additional hydroxy group at C-5 gives a further hydrogen bond with His151. These data are in perfect

https://dx.doi.org/10.1021/acs.jnatprod.0c01387
J. Nat. Prod. 2021, 84, 654−665

agreement with the higher inhibitory activity of **1** and especially **2** with respect to **3** (see Tables 5 and 6). The compounds **7** (Figure 5c) and **9**, hydroxylated derivatives of daidzein (**1**) and formononetin (**3**), respectively, showed better affinity for PL than the parent compounds thanks to the new OH groups. In fact, the OH at C-3′ in **7** establishes a further hydrogen bond with Phe215; analogously, the OH at C-8 in **9** forms two hydrogen bonds with Phe77 and His151. The observed interactions highlight the importance of the phenolic groups for PL affinity. Furthermore, it is worth noting that the catechol group in compound **7** improves its overall interaction with the protein. On the other hand, the OMe group at C-4′ of **3** (Figure 5b) and **9** does not establish any interaction with the amino acid residues of catalytic pocket.

In general, the brominated isoflavones **10** and **12** (Figure S36) present almost the same interactions observed for the natural leads, forming a more stable complex for the polarization effect caused by bromine groups.

As a confirmation that the presence of OH groups in isoflavones improves the interaction with PL, the docking study showed that the permethylated (**13**) and peracetylated (**14**) derivatives of isoflavone **7** have a lower affinity with the PL catalytic site than the parent compound, due to the lack of free OH groups. Also these results are in perfect agreement with the very low inhibitory activity observed for **13** and **14**.

It is worth noting that the residues Ser152 and His263 are part of the catalytic triad, and in particular, Ser152 is believed to play a pivotal role in the catalytic activity of PL.[33] Hence, on the basis of docking data, the isoflavones under study could have a role as competitive inhibitors. These findings are not in contrast with the above-discussed kinetic data. In fact, notwithstanding, Lineweaver−Burk plots indicated that genistein (**2**) is the only competitive inhibitor, and **1**, **3**, **10**, and **11** resulted in mixed inhibitors; the latter showed an affinity for the PL catalytic site (similarly to a competitive inhibitor) greater than for the PL−substrate complex.

In conclusion, in this work, a detailed study on inhibition of the pancreatic lipase activity by natural isoflavones and semisynthetic derivatives has been carried out for the first time. The above-reported results highlight the subclass of isoflavones as promising polyphenols for the development of potential antiobesity agents. An in vitro lipase inhibition assay showed that the natural isoflavone **2** is the most potent PL inhibitor. However, hydroxylation and bromination resulted in advantageous modifications for improving the PL inhibitory activity of isoflavones, as confirmed by intrinsic fluorescence and kinetic measurements. The docking study pointed out the molecular interactions involved between the isoflavones and the PL catalytic site, thus supporting our findings.

EXPERIMENTAL SECTION

General Experimental Procedures. UV−vis spectra were acquired with a Jasco V630 spectrophotometer using a 1 cm quartz cuvette at 27 °C and in the range 200−600 nm.

NMR spectra were run on a Varian Unity Inova spectrometer operating at 499.86 (^{1}H) and 125.70 MHz (^{13}C). All NMR experiments, including 2D spectra, g-COSY, g-HSQCAD, and g-HMBCAD, were acquired at constant temperature (27 °C). g-HMBCAD experiments were optimized for a long-range ^{13}C−^{1}H coupling constant of 8.0 Hz. Chemical shifts are indirectly referred to tetramethylsilane using residual solvent signals at 2.50 ppm for DMSO-d_6 and 7.26 ppm for chloroform-*d*.

High-resolution mass spectra (HRMS) were acquired with an Orbitrap Fusion Tribrid (Q-OT-qIT) mass spectrometer (Thermo Fisher Scientific) equipped with an ESI ion source. Mass data were acquired on samples directly infused and volatilized using the optimized parameters previously described.[40]

The lipase inhibition assay was performed on a 96-well microplate, and the UV−vis measurements were done on a Synergy H1 microplate reader (BioTek) at 405 nm. Kinetic measurements were carried out on a Synergy H1 microplate reader (BioTek) under the same conditions reported for PL inhibition; optical density measurements were acquired every minute for 30 min. Intrinsic fluorescence experiments were performed on an Agilent Cary Eclipse spectrometer. Fluorescence spectra were acquired in the range 315−500 nm, setting the following parameters: λ_{EXC} at 285 nm and excitation and emission slits of 10 nm. Experiments were carried out at 27, 32, and 37 °C.

Unless otherwise stated, all solvents and reagents were purchased from commercial sources; they were analytically pure and for spectroscopy use. Daidzein, genistein, and formononetin were purchased from TCI Europe N. V. *p*-Nitrophenyl butyrate, porcine pancreatic lipase (PL; Type II), and orlistat were purchased from Merck. IBX was prepared before use, as previously reported.[21]

Synthesis of Isoflavones 7 and 8. *Typical Procedure for the Two-Step Synthesis of the Isoflavones 7 and 8.* For step 1, Resorcinol (**4**; 102.2 mg; 0.93 mmol) or orcinol (**5**; 115.1 mg; 0.93 mmol) was treated with 3,4-dihydroxy-phenylacetic acid (**6**; 153.5 mg; 0.93 mmol) and a 46.5% $BF_3{\cdot}Et_2O$ solution (2.1 mL; 7.5 mmol). The mixture was heated at 110 °C under N_2 for 1.5 h. The crude was cooled to rt and treated with cold H_2O (20 mL). The deoxybenzoin **4a** was recovered by precipitation, whereas the intermediate **5a** was recovered by partitioning the aqueous phase with Et_2O (3 × 10 mL). The combined organic layer was successively partitioned with saturated $NaHCO_3$ (2 × 20 mL), washed with H_2O (30 mL), dried over anhydrous Na_2SO_4, and concentrated in vacuo.

For step 2, the deoxybenzoin (**4a** or **5a**; 0.12 mmol) was dissolved in dry DMF (0.2 mL), and a solution of $MeSO_2Cl$ (0.12 mL in 0.6 mL of dry DMF; Vilsmeier reagent), prepared separately, was added. The mixtures were stirred at 80 °C under N_2 atmosphere for 1.5 h and then at 40 °C overnight. In another experiment, the deoxybenzoin **4a** (0.12 mmol) was treated as described above, but an aliquot of 46.5% $BF_3{\cdot}Et_2O$ solution (0.15 mL; 0.52 mmol) was added before the addition of Vilsmeier reagent. The mixtures were diluted with a 12% AcONa solution (20 mL), and they were partitioned with EtOAc (3 × 10 mL). The combined organic layer was washed with water, dried over anhydrous Na_2SO_4, and evaporated until dry.

Typical Procedure for the One-Pot Synthesis of the Isoflavones 7 and 8. Resorcinol (**4**; 500.1 mg; 4.54 mmol) or orcinol (**5**; 563.4 mg; 4.54 mmol) was mixed with 3,4-dihydroxyphenylacetic acid (**6**; 763.4 mg; 4.54 mmol), and a 46.5% $BF_3{\cdot}Et_2O$ solution (9.7 mL; 34.3 mmol) was added. The mixture was heated at 110 °C under N_2 atmosphere for 2 h. Separately, a solution of $MeSO_2Cl$ (4.5 mL in 22 mL of dry DMF; Vilsmeier reagent) was prepared and stirred at rt for 30 min. When the mixture containing the deoxybenzoin was cooled down, the Vilsmeier reagent was added in three times. Then the mixture was heated at 80 °C for 1.5 h, and finally, it was stirred at rt overnight. The mixtures were diluted with a 12% AcONa solution (100 mL), and they were partitioned with EtOAc (3 × 40 mL). The combined organic layer was washed with H_2O (100 mL), dried over anhydrous Na_2SO_4, and evaporated until dry.

The two isoflavones were recovered from the organic crude after column chromatography on silica gel was eluted with CH_2Cl_2:MeOH (100:0 → 85:15).

3-(3,4-Dihydroxyphenyl)-7-hydroxy-4H-chromen-4-one (7). There is a 42−57% yield from two-step synthesis and 94% yield from one-pot reaction. R_f (TLC) = 0.30 (93:7 CH_2Cl_2:MeOH). UV (50:50 CH_3OH:H_2O) $\lambda_{max}(\log\varepsilon)$ = 254 (4.32), 403 (1.65) nm. The spectroscopic data were in agreement with those reported in the literature.[28]

https://dx.doi.org/10.1021/acs.jnatprod.0c01387
J. Nat. Prod. 2021, 84, 654−665

*3-(3,4-Dihydroxyphenyl)-7-hydroxy-5-methyl-4H-chromen-4-one (**8**).* There is a 16% yield from two-steps synthesis and 37% yield from one-pot reaction. R_f (TLC) = 0.72 (93:7 CH_2Cl_2:MeOH). ^1H, ^{13}C, and HMBC NMR (Table 2). HRMS (ESI−) *m/z* 283.0628 $[M - H]^-$ (calcd for $C_{16}H_{11}O_5$, 283.0606).

Hydroxylation of Isoflavones 1 and 3. The preliminary experiments are reported in the Supporting Information.

*Synthesis of **7**.* Daidzein (15 mg; 0.06 mmol) was dissolved in DMSO (0.6 mL) and treated with IBX (20.2 mg; 0.07 mmol) at 50 °C for 2 h. Then, the mixture was quenched by adding a saturated $Na_2S_2O_4$ solution (0.6 mL), and the mixture was stirred at rt for 5 min. The mixture was diluted to 5 mL, and it was partitioned with EtOAc (3 × 5 mL). The organic layer was washed with H_2O, dried over anhydrous Na_2SO_4, and taken to dryness. The column chromatography on silica gel eluting with CH_2Cl_2:MeOH (from 100:0 → 90:10) afforded **7** with 28% yield. Spectroscopic data were in agreement with those reported in the literature.[28]

*Synthesis of Retusin (**9**).* Formononetin (100.2 mg, 0.37 mmol) was dissolved in DMSO (3.5 mL), and IBX (124.7 mg; 0.44 mmol) was added. Then, the reaction was treated with 4 mL of a saturated $Na_2S_2O_4$ solution at rt for 5 min. The mixture was diluted to 15 mL, and it was partitioned with EtOAc (3 × 15 mL). The organic layer was washed with H_2O and dried over anhydrous Na_2SO_4, and the solvent was evaporated until dryness. The column chromatography on silica gel eluting with *n*-hexane:acetone (from 100:0 → 50:50) afforded **9** with 43% yield. R_f (TLC) = 0.42 (60:40 *n*-hexane:acetone). UV (50:50 MeOH:H_2O) λ_{max}(log ε) = 259 (4.53), 305 (3.92) nm. Spectroscopic data were in agreement with those reported in the literature.[26]

Bromination of Isoflavones 1 and 3. For bromination of **1** and **3**, some preliminary screenings were performed as follows:

(1) Compound **3** (4.0 mg; 0.015 mmol) was stirred with CH_3COOH (75 μL), NaBr (1.5 mg; 0.015 mmol), and 30% H_2O_2 (50 μL; 0.044 mmol) at rt for 6 h;
(2) Compound **3** (4.0 mg; 0.015 mmol) was stirred with CH_3COOH (75 μL), NaBr (1.5 mg; 0.015 mmol), and oxone (11.2 mg; 0.017 mmol, previously dissolved in 50 μL of water) at rt for 6 h;
(3) Compound **3** (4.0 mg; 0.015 mmol) was dissolved with CH_3COOH (75 μL), and a Br_2 solution (1 μL; 0.017 mmol; in 850 μL of CH_3CN) was dropwise added; the mixture was mixed at rt for 40 min;
(4) Compound **3** (3 mg; 0.011 mmol) was dissolved in $CHCl_3$ (0.115 mL) and MeOH (20 μL); then, a Br_2 solution (0.6 μL; 0.011 mmol in 450 μL of $CHCl_3$) was dropwise added, and the mixture was kept at 0 °C for 1 h;
(5) Compound **1** (20 mg; 0.08 mmol) was dissolved in $CHCl_3$ (1.2 mL) and MeOH (0.1 mL); then, a Br_2 solution (4.0 μL; 0.08 mmol; in 3.5 mL of $CHCl_3$) was dropwise added, and the mixture was kept at 0 °C for 3 h.

The reactions were monitored by TLC, and they were quenched by addition of a saturated $Na_2S_2O_3$ solution (1 mL). The crude was partitioned with $CHCl_3$ (3 × 1 mL), and the organic layer was washed with H_2O, dried over anhydrous Na_2SO_4, and taken to dryness.

*Synthesis of 8-Bromo-3-(3,5-dibromo-4-hydroxyphenyl)-7-hydroxy-4H-chromen-4-one (**10**).* Daidzein (**1**; 100 mg; 0.39 mmol) was solubilized with $CHCl_3$: MeOH 90:10 (6 mL) and stirred in an ice bath. A Br_2 solution (20 μL; 0.39 mmol) in $CHCl_3$ (17 mL), freshly prepared, was added dropwise to **1**. After 3 h, the reaction was quenched by addition of a saturated $Na_2S_2O_3$ solution (15 mL). The crude was partitioned with $CHCl_3$ (3 × 15 mL); the total organic layer was washed with H_2O (30 mL), and dried over anhydrous Na_2SO_4. The solvent was evaporated until dryness. The isoflavone **10** was recovered with 70% yield after column chromatography on silica gel and eluting with *n*-hexane:acetone (90:10 → 60:40). R_f(TLC) = 0.46 (60:40 *n*-hexane/acetone). Spectroscopic data were in agreement with those reported in the literature.[30]

*Synthesis of 8-Bromo-7-hydroxy-3-(4-methoxyphenyl)-4H-chromen-4-one (**11**).* Formononetin (**3**; 200 mg; 0.74 mmol) was solubilized with $CHCl_3$:MeOH 90:10 (9.5 mL), and the solution was kept in an ice bath. A freshly prepared Br_2 solution (40 μL; 0.74 mmol; in 32 mL of $CHCl_3$) was poured dropwise to **3**. The mixture was stirred at 0 °C, and after 4.5 h, a saturated solution of $Na_2S_2O_3$ (20 mL) was added. The two phases were separated, and the aqueous phase was partitioned with $CHCl_3$ (3 × 20 mL). The organic layer was washed with H_2O and dried over anhydrous Na_2SO_4, and the solvent was evaporated until dry. The isoflavone **11** was obtained with 80% yield without further purification. R_f (TLC) = 0.64 (95:5 CH_2Cl_2:MeOH). UV (50:50 MeOH:H_2O) λ_{max}(log ε) = 261 (4.26), 340 (3.75) nm. ^1H and ^{13}C NMR, Table 4. HRMS (ESI−) *m/z* 344.9781 $[M - H]^-$ (100) (calcd for $C_{16}H_{10}{}^{79}BrO_4$, 344.9762) and 346.9762 $[M - H]^-$ (97) (calcd for $C_{16}H_{10}{}^{81}BrO_4$, 346.9742).

*Synthesis of 8-Bromo-3-(3-bromo-4-methoxyphenyl)-7-hydroxy-4H-chromen-4-one (**12**).* Formononetin (**3**; 100 mg; 0.37 mmol) was solubilized with glacial acetic acid (1.5 mL). A freshly prepared Br_2 solution (20 μL; 0.44 mmol; in 16 mL of CH_3CN) was added dropwise to **3**. The mixture was stirred at rt, and after 40 min, the reaction was quenched by addition of a saturated solution of $Na_2S_2O_3$ (10 mL). The crude was partitioned with $CHCl_3$ (3 × 20 mL). The organic layer was washed with water and dried over anhydrous Na_2SO_4, and the solvent was evaporated until dry. The isoflavone **12** was obtained with 92% yield without further purification. R_f (TLC) = 0.50 (97:3 CH_2Cl_2:MeOH). UV (50:50 MeOH:H_2O) λ_{max}(log ε) = 255 (4.21), 344 (3.69) nm. ^1H and ^{13}C NMR, Table 4. HRMS (ESI−) (1:2:1 ratio) *m/z* 422.8895 $[M - H]^-$ (calcd for $C_{16}H_9{}^{79}Br_2O_4$, 422.8867), 424.8873 $[M - H]^-$ (100) (calcd for $C_{16}H_9{}^{79}Br^{81}BrO_4$, 424.8847), 426.8852 $[M - H]^-$ (50) (calcd for $C_{16}H_9{}^{81}Br_2O_4$, 426.8827).

Synthesis of Derivatives of 7. *Synthesis of Cabreuvine (**13**).* The isoflavone **7** (40.2 mg; 0.14 mmol) was dissolved in dry acetone (3 mL), and it was stirred with anhydrous K_2CO_3 (174.7 mg;1.23 mmol) at rt for 10 min. Then, CH_3I (85 μL; 1.23 mmol) was added to the reaction flask, and the mixture was refluxed for 24 h. After 5 h, another aliquot of CH_3I (20 μL, 0.32 mmol) was added. The expected product was recovered after filtration and distillation of the solvent by rotavapor with 52% yield. R_f (TLC) = 0.80 (96:4 CH_2Cl_2:MeOH). UV (50:50 MeOH:H_2O) λ_{max}(log ε) = 250 (4.52), 304 (4.02) nm. NMR spectroscopic data of **13** were in agreement with those reported in the literature for cabreuvin.[31]

*Synthesis of 4-(7-Acetoxy-4-oxo-4H-chromen-3-yl)-1,2-phenylene diacetate (**14**).* The isoflavone **7** (40.9 mg; 0.14 mmol) was solubilized with $CHCl_3$ (200 μL), and it was mixed with anhydrous K_2CO_3 (76.7 mg; 0.56 mmol) and acetic anhydride (55 μL; 0.6 mmol) at rt for 19 h. The mixture was partitioned with EtOAc (3 × 20 mL), and the combined organic layer was washed with H_2O and dried over anhydrous Na_2SO_4; the solvent was evaporated until dry. Column chromatography on diol silica gel eluted with *n*-hexane:CH_2Cl_2 (20:80 → 0:100) furnished the acetylated isoflavone **14** with 51.0% yield. R_f(TLC) = 0.37 (98:2 CH_2Cl_2/MeOH). UV (50:50 MeOH:H_2O) λ_{max}(log ε) = 248 (4.67), 303 (4.08) nm. The ^1H and ^{13}C NMR data are listed in Table 4. HRMS (ESI+) *m/z* 419.0780 $[M + Na]^+$ (calcd for $C_{21}H_{16}NaO_8$, 419.0743).

Measurements of Lipase Inhibition. The PL inhibition assay was performed adopting the conditions previously reported.[33,41] Briefly, in a 96-well microplate, 150 μL of phosphate buffer (50 mM, pH = 7.2), the PL solution (300 U/mL in phosphate buffer; 15 μL), and different aliquots (2, 4, 6, 8, 10, and 15 μL) of tested compounds (stock solutions ranging from 1 mM to 5 mM were prepared in MeOH or MeOH:DMSO 95:5) or of orlistat (6.7 μM in buffer) were mixed. The reactions were incubated at 37 °C for 10 min. Then, the substrate *p*-nitrophenyl butyrate (3.2 mM in H_2O:DMF 70:30, 10 μL) was added, and the microplate was incubated at 37 °C for 30 min under moderate shaking. The plate measurements were acquired at 405 nm. The assays were performed in triplicate with five different concentrations for each compound. The amount of MeOH or DMSO used in the experiment did not affect the lipase inhibitory

https://dx.doi.org/10.1021/acs.jnatprod.0c01387
J. Nat. Prod. 2021, 84, 654−665

activity. The inhibition percentage was calculated by the following equation:

$$\text{inhibition } \% = \frac{(A_{\text{control}} - A_{\text{sample}})}{A_{\text{control}}} \times 100 \quad (1)$$

where A_{control} is the absorbance measured for the mixture enzyme/substrate (without tested compounds) and A_{sample} is the absorbance measured in the same conditions and in the presence of the tested compounds. The concentration required to inhibit the 50% activity of the enzyme (IC_{50}) was calculated by regression analysis.

Fluorescence Spectra Measurements. The interaction between the isoflavones and PL was performed by fluorimetric titration. For each tested compound, the experiments (each in triplicate) were performed at 27, 32, and 37 °C. The PL (1.1 μM in 0.1 M phosphate buffer containing 0.1 M NaCl, pH 7.4; 2 mL) was titrated by successive additions (1 or 2 μL) of the tested compounds. The fluorescence spectrum was acquired 1 min after each addition from 310 to 500 nm. The concentration of starting solution of the isoflavones were chosen on the basis of the IC_{50} values. The fluorescence at the maximum intensity was employed to obtain the Stern–Volmer plots according eqs 2 and 3:[35]

$$\frac{F_o}{F} = 1 + K_{SV}[Q] = 1 + K_q\tau_0[Q] \quad (2)$$

$$\log \frac{F_0 - F}{F} = \log K_a + n\log [Q] \quad (3)$$

F_0 and F are the fluorescence intensities of enzyme before and after the addition of quencher, respectively. [Q] represents the concentration of the isoflavones studied. τ_0 is the average life of protein, and it was reported to be 1.59×10^{-9} s.[42] K_{SV} and K_q represent the quenching constant and the quenching rate constant, respectively. K_a is the binding constant, and n is the number of binding sites.

Kinetics of Lipase Inhibition. The mode of inhibition of PL in the presence of tested isoflavones was determined by elaboration of UV–vis spectroscopic data with Lineweaver–Burk plots. The experiments were performed in 96-well plates employing the enzyme (120 U/mL in phosphate buffer; 10 μL), the selected isoflavones, and the increasing concentrations of the substrate *p*-nitrophenyl butyrate (from 0.3 to 1.9 mM) in a final volume of 200 μL. Optimal concentration of the tested isoflavones were chosen on the basis of the IC_{50} values. The absorbance was read at 405 nm every 1 min for 30 min at 37 °C.

The inhibition constants were calculated from the equations

$$v_0 = \frac{v_{\max}S}{K_m\left(1 + \frac{I}{K_i}\right) + S} \quad (4)$$

$$v_0 = \frac{v_{\max}S}{K_m\left(1 + \frac{I}{K_i}\right) + S\left(1 + \frac{I}{K'_i}\right)} \quad (5)$$

for competitive and mixed-type inhibitors, respectively, where v_0 is the initial velocity in the absence and presence of the inhibitor, S and I are the concentrations of substrate and inhibitor, respectively, $v_{\max}$ is the maximum velocity, K_m is the Michaelis–Menten constant, K_i is the competitive inhibition constant, and K'_i is the uncompetitive inhibition constant.

The graphs of slope and *y*-intercept of Lineweaver–Burk plots versus the inhibitor concentration gave a straight line, whose intercept corresponds to K_i and K'_i values, respectively.[43]

Data Analysis. Results of the above-reported experiments were obtained by plotting the experimental measurements on OriginPro 2018 or Microsoft Excel 2016 and were expressed as means ± SD. Statistical analysis was performed using one-way analysis of variance (ANOVA), and differences were designated as statistically significant when $p < 0.05$.

Molecular Docking Analysis. The .sdf files of orlistat, genistein, daidzein, and formononetin were downloaded from Pubchem (https://pubchem.ncbi.nlm.nih.gov/, ID codes, respectively, are 3034010, 5280961, 5281708, and 5280378). Meanwhile, the other ligands, namely, the isoflavones **7**–**14** were drawn by Chemdraw and saved in .sdf files. The 3D models were geometrically minimized with optimized potential liquid simulation (OPLS3) force fields[44] considering the protonation state at pH of 7.0 ± 1 and processed using LigPrep interfaced with Maestro (Version 11) of Schröedinger suite.[45] The minimized geometries were converted in .pdbqt files by Autodock Tools (1.5.6).

The 3D structure of pancreatic lipase (PDB ID: 1LPB) was downloaded from Protein Data Bank.[46] The lipase is cocrystallized with colipase in the presence of methoxy undecyl phosphonic (MUP) as inhibitor and β-octylglucoside (BOG) as surfactant. Protein was prepared with Protein wizard, MUP, and BOG, and H_2O molecules were removed; then, the .pdb file obtained was processed with Autodock Tools 1.5.6 and converted in .pdbqt file, merging nonpolar hydrogens and adding Gasteiger charges. The molecular docking studies were performed using Autodock4 (AD4)[37] and Autodock Vina software 1.5.6.[38,39] Autogrid4 (4.2.6 version) was used to generate the gridmaps. The grid box was centered in the binding site of protein, with grid coordinates of 50 × 40 × 50 Å^3 for *x*, *y*, and *z*, respectively. The spacing between the grid coordinates was 0.708 Å. The grid center was set to 7.500, 26.042, and 47.696 Å. For the docking experiments carried out with AD4, The Lamarckian Genetic Algorithm (LGA) was chosen to search for the best conformers. During the docking process, a maximum of 10 conformers was considered for each ligand. AD4 GA parameters are set as default: ga_pop_size = 150, ga_num_evals = 2 500 000, ga_num_generations = 27 000, ga_elitism = 1, ga_mutation_rate = 0.02, ga_crossover_rate = 0.8, ga_cauchy_alpha = 0.0, ga_cauchy_beta = 1.0. The docking carried out with autodock Vina was set with exhaustiveness and energy difference as default (8 and 3 respectively) and saving 9 conformations as the maximum number of binding mode. In Docking calculation, ligands were treated as flexible, and protein were treated as rigid. AD4 and autodock Vina were compiled and run in OSX Yosemite (10.10.5) environment. The analysis of docking outcomes were carried out by Autodock Tool (1.5.6), and figures of 3D models were generated by Pymol (2.3.5).

■ ASSOCIATED CONTENT

Supporting Information

The Supporting Information is available free of charge at https://pubs.acs.org/doi/10.1021/acs.jnatprod.0c01387.

Experimental details for preliminary hydroxylation reactions of **1**–**3**; preliminary experiments of bromination of **2**; HRMS, ^{1}H, ^{13}C, and 2D NMR spectra of new compounds **8**, **11**, **12**, and **14**; fluorescence spectra of PL in presence of **1**–**3**, **10**, and **11**; and list of binding energy and noncovalent interactions between isoflavones **1**–**3**, **7**–**14**, and PL (PDF)

■ AUTHOR INFORMATION

Corresponding Authors

Corrado Tringali − *Dipartimento di Scienze Chimiche, Università degli Studi di Catania, 95125 Catania, Italy;* orcid.org/0000-0003-4268-0115; Phone: +39 0957385025; Email: ctringali@unict.it; Fax: +39 095580138

Nunzio Cardullo − *Dipartimento di Scienze Chimiche, Università degli Studi di Catania, 95125 Catania, Italy;* orcid.org/0000-0003-1480-0861; Email: ncardullo@unict.it

https://dx.doi.org/10.1021/acs.jnatprod.0c01387
J. Nat. Prod. 2021, 84, 654−665

Authors

Vera Muccilli − *Dipartimento di Scienze Chimiche, Università degli Studi di Catania, 95125 Catania, Italy;* orcid.org/0000-0002-6212-5154

Luana Pulvirenti − *Dipartimento di Scienze Chimiche, Università degli Studi di Catania, 95125 Catania, Italy*

Complete contact information is available at: https://pubs.acs.org/10.1021/acs.jnatprod.0c01387

Notes

The authors declare no competing financial interest.

■ ACKNOWLEDGMENTS

This research was funded by the by MIUR ITALY PRIN 2017 (Project No. 2017A95NCJ). The authors acknowledge the Bio-Nanotech Research and Innovation Tower (BRIT) of University of Catania for the availability of the Synergy H1 microplate reader.

■ DEDICATION

Dedicated to Dr. A. Douglas Kinghorn, The Ohio State University, for his pioneering work on bioactive natural products.

■ REFERENCES

(1) World Health Organization. Fact Sheet Obesity and Overweight. https://www.who.int/news-room/fact-sheets/detail/obesity-and-overweight/ (accessed October 2020).
(2) Liu, T. T.; Liu, X. T.; Chen, Q. X.; Shi, Y. *Biomed. Pharmacother.* **2020**, *128*, 110314.
(3) Sergent, T.; Vanderstraeten, J.; Winand, J.; Beguin, P.; Schneider, Y.-J. *Food Chem.* **2012**, *135*, 68−73.
(4) Birari, R. B.; Bhutani, K. K. *Drug Discovery Today* **2007**, *12*, 879−889.
(5) Seyedan, A.; Alshawsh, M. A.; Alshagga, M. A.; Koosha, S.; Mohamed, Z. *Evidence-Based Complementary and Alternative Medicine* **2015**, *2015*, 1−13.
(6) Yung Cheung, B. M.; Tsang Cheung, T.; Samaranayake, N. R. *Ther. Adv. Drug Saf.* **2013**, *4*, 171−181.
(7) Buchholz, T.; Melzig, M. F. *Planta Med.* **2015**, *81*, 771−783.
(8) Yun, J. W. *Phytochemistry* **2010**, *71*, 1625−1641.
(9) Martinez-Gonzalez, A. I.; Alvarez-Parrilla, E.; Diaz-Sanchez, A. G.; de la Rosa, L. A.; Nunez-Gastelum, J. A.; Vazquez-Flores, A. A.; Gonzalez-Aguilar, G. A. *Food Technol. Biotechnol.* **2017**, *55*, 519−530.
(10) Weibel, E. K.; Hadvary, P.; Hochuli, E.; Kupfer, E.; Lengsfeld, H. *J. Antibiot.* **1987**, *40*, 1081−1085.
(11) Hochuli, E.; Kupfer, E.; Maurer, R.; Meister, W.; Mercadal, Y.; Schmidt, K. *J. Antibiot.* **1987**, *40*, 1086−1091.
(12) Laura de la Garza, A.; Milagro, F. I.; Boque, N.; Campion, J.; Alfredo Martinez, J. *Planta Med.* **2011**, *77*, 773−785.
(13) Goncalves, R.; Mateus, N.; De Freitas, V. *J. Agric. Food Chem.* **2010**, *58*, 11901−11906.
(14) Vitale, D. C.; Piazza, C.; Melilli, B.; Drago, F.; Salomone, S. *Eur. J. Drug Metab. Pharmacokinet.* **2013**, *38*, 15−25.
(15) Yu, J.; Bi, X. J.; Yu, B.; Chen, D. W. *Nutrients* **2016**, *8*, 361.
(16) Andres, S.; Abraham, K.; Appel, K. E.; Lampen, A. *Crit. Rev. Toxicol.* **2011**, *41*, 463−506.
(17) Umeno, A.; Horie, M.; Murotomi, K.; Nakajima, Y.; Yoshida, Y. *Molecules* **2016**, *21*, 708.
(18) Wang, D. M.; Hu, M.; Li, X. P.; Zhang, D.; Chen, C. J.; Fu, J. M.; Shao, S.; Shi, G. N.; Zhou, Y.; Wu, S.; Zhang, T. T. *Eur. J. Med. Chem.* **2019**, *168*, 207−220.
(19) Shimura, S.; Itoh, Y.; Yamashita, A.; Kitano, A.; Hatano, T.; Yoshida, T.; Okuda, T. *Nippon Shokuhin Kogyo Gakkaishi* **1994**, *41*, 847−850.
(20) Mu, Y.; Kou, T.; Wei, B.; Lu, X.; Liu, J.; Tian, H.; Zhang, W.; Liu, B.; Li, H.; Cui, W.; Wang, Q. *Nutrients* **2019**, *11*, 2790.
(21) Akhlaghi, M.; Zare, M.; Nouripour, F. *Adv. Nutr.* **2017**, *8*, 705−717.
(22) Ørgaard, A.; Jensen, L. *Exp. Biol. Med.* **2008**, *233*, 1066−1080.
(23) Cardullo, N.; Spatafora, C.; Musso, N.; Barresi, V.; Condorelli, D.; Tringali, C. *J. Nat. Prod.* **2015**, *78*, 2675−2683.
(24) Pulvirenti, L.; Muccilli, V.; Cardullo, N.; Spatafora, C.; Tringali, C. *J. Nat. Prod.* **2017**, *80*, 1648−1657.
(25) Cardullo, N.; Catinella, C.; Floresta, G.; Muccilli, V.; Rosselli, S.; Rescifina, A.; Bruno, M.; Tringali, C. *J. Nat. Prod.* **2019**, *82*, 573−582.
(26) Yadav, S. K. *Int. J. Org. Chem.* **2014**, *4*, 236−246.
(27) Balasubramanian, S.; Nair, M. G. *Synth. Commun.* **2000**, *30*, 469−484.
(28) Goto, H.; Terao, Y.; Akai, S. *Chem. Pharm. Bull.* **2009**, *57*, 346−360.
(29) Barontini, M.; Bernini, R.; Crisante, F.; Fabrizi, G. *Tetrahedron* **2010**, *66*, 6047−6053.
(30) Lee, S. R.; Schalk, F.; Schwitalla, J. W.; Benndorf, R.; Vollmers, J.; Kaster, A.-K.; de Beer, Z. W.; Park, M.; Ahn, M.-J.; Jung, W. H.; Beemelmanns, C.; Kim, K. H. *J. Nat. Prod.* **2020**, *83*, 3102−3110.
(31) Ndemangou, B.; Sielinou, V. T.; Vardamides, J. C.; Ali, M. S.; Lateef, M.; Iqbal, L.; Afza, N.; Nkengfack, A. E. *J. Enzyme Inhib. Med. Chem.* **2013**, *28*, 1156−1161.
(32) Funayama, S.; Anraku, Y.; Mita, A.; Komiyama, K.; Omura, S. *J. Antibiot.* **1989**, *42*, 1350−1355.
(33) Roh, C.; Jung, U. *Int. J. Mol. Sci.* **2012**, *13*, 1710−1719.
(34) van der Weert, M.; Stella, L. *J. Mol. Struct.* **2011**, *998*, 144−150.
(35) Cardullo, N.; Muccilli, V.; Pulvirenti, L.; Cornu, A.; Pouysegu, L.; Deffieux, D.; Quideau, S.; Tringali, C. *Food Chem.* **2020**, *313*, 126099.
(36) Li, Y. Q.; Zhou, F. C.; Gao, F.; Bian, J. S.; Shan, F. *J. Agric. Food Chem.* **2009**, *57*, 11463−11468.
(37) Mohapatra, S.; Prasad, A.; Haque, F.; Ray, S.; De, B.; Ray, S. S. *J. Appl. Pharm. Sci.* **2015**, *5*, 042−047.
(38) Vu, H. M. T.; Vu, D. D.; Truong, V. D.; Nguyen, T. V. P.; Tran, T. D. *MedPharmRes.* **2017**, *1*, 26−36.
(39) Tang, W.-Z.; Liu, J.-T.; Hu, Q.; He, R.-J.; Guan, X.-Q.; Ge, G.-B.; Han, H.; Yang, F.; Lin, H.-W. *J. Nat. Prod.* **2020**, *83*, 2287−2293.
(40) Cardullo, N.; Barresi, V.; Muccilli, V.; Spampinato, G.; D'Amico, M.; Condorelli, D. F.; Tringali, C. *Molecules* **2020**, *25*, 733.
(41) Slanc, P.; Doljak, B.; Kreft, S.; Lunder, M.; Janes, D.; Strukelj, B. *Phytother. Res.* **2009**, *23*, 874−877.
(42) Nasri, R.; Bidel, L. P. R.; Rugani, N.; Perrier, V.; Carriere, F.; Dubreucq, E.; Jay-Allemand, C. *Molecules* **2019**, *24*, 2888.
(43) Meiering, S.; Inhoff, O.; Mies, J.; Vincek, A.; Garcia, G.; Kramer, B.; Dormeyer, M.; Krauth-Siegel, R. L. *J. Med. Chem.* **2005**, *48*, 4793−4802.
(44) Harder, E.; Damm, W.; Maple, J.; Wu, C.; Reboul, M.; Xiang, J. Y.; Wang, L.; Lupyan, D.; Dahlgren, M. K.; Knight, J. L.; Kaus, J. W.; Cerutti, D. S.; Krilov, G.; Jorgensen, W.; Abel, R.; Friesner, R. A. *J. Chem. Theory Comput.* **2016**, *12*, 281−296.
(45) *Schrodinger Release 2017-1, LigPrep*; Schrodinger, LLC: New York, NY, 2017.
(46) RCSB. Protein Data Bank. https://www.rcsb.org/structure/1lpb (accessed April 2020).